

## A simple electrokinetic protein preconcentrator utilizing nano-interstices

Yu-Hung Chen,<sup>1,2,a)</sup> Hsuan Franziska Wu,<sup>1</sup> Tamara G. Amstislavskaya,<sup>3</sup>  
 Chang-Yu Li,<sup>4</sup> and Chun-Ping Jen<sup>4,a)</sup>

<sup>1</sup>*Department of Medicine, College of Medicine, National Cheng Kung University,  
 Tainan, Taiwan*

<sup>2</sup>*Department of Biochemistry and Molecular Biology, College of Medicine,  
 National Cheng Kung University, Tainan, Taiwan*

<sup>3</sup>*Laboratory of Experimental Models of Emotional Pathology, Scientific Research Institute  
 of Physiology and Basic Medicine, Novosibirsk, Russia*

<sup>4</sup>*Department of Mechanical Engineering, National Chung Cheng University, Chia Yi,  
 Taiwan*

(Received 7 February 2016; accepted 1 April 2016; published online 12 April 2016)

This work proposes a simple method for creating nanofluidic channels for protein preconcentration through self-assembled gold nanoparticles (AuNPs) using the exclusion-enrichment effect. A depletion force is elicited in nano-interstices among self-assembled AuNPs due to the overlap of electrical double layers (EDLs); therefore, proteins quickly accumulate. The experimental results show that the generation of depletion forces is correlated with the size of the AuNPs. The self-assembled monolayer of AuNPs (13 nm in diameter) can successfully preconcentrate proteins through effective EDL overlapping. This approach provides a new process to produce nanochannels that does not require high-voltage or time-consuming fabrication. Published by AIP Publishing. [<http://dx.doi.org/10.1063/1.4946768>]

### I. INTRODUCTION

Preconcentration of low-concentration proteins is employed to increase the sensitivity and accuracy of biochemical analyses. Particle concentration had been done adopting the optoelectrokinetic technique, termed rapid electrokinetic patterning (REP).<sup>1,2</sup> With an electric field and a focused laser beam applying on the microchip simultaneously, the immunocomplexes in the droplet of sample were further concentrated to enhance the Förster resonance energy transfer (FRET) fluorescent signal.<sup>2</sup> This approach is relative complicated and the rising of temperature might damage the analytes. A nonlinear electrokinetic flow is induced in a nanofluidic channel due to the overlap of electrical double layers (EDLs), resulting in the fast accumulation of proteins, referred to as the exclusion-enrichment effect.<sup>3</sup> A new class of ion concentration polarization mechanism called “capillarity ion concentration polarization” (CICP) was reported.<sup>4</sup> The capillary force of the perm-selective hydrogel spontaneously generated an ion depletion zone in a microfluidic channel by selectively absorbing counter-ions in a sample solution instead of an external electrical voltage source was investigated. However, the efficiency was lower than that of conventional electrokinetic ion concentration polarization operation due to the absence of a drift ion migration. Moreover, a dynamic methodology for quantifying the pre-concentration dynamics of particles under an electrokinetic force balance, driven by negative dielectrophoresis (nDEP) away from insulating constriction tips, which causes a highly delocalized pre-concentration zone has been presented by Rohani *et al.*<sup>5</sup> They employed a statistical description of particle distribution across the device geometry to determine threshold intensity levels for preconcentration and depletion, thus the region of interest was being defined dynamically. Nanofluidic channels can be

<sup>a)</sup>Authors to whom correspondence should be addressed. Electronic addresses: second@mail.ncku.edu.tw and imecpj@ccu.edu.tw.

fabricated to create the exclusion-enrichment effect, and simple buffer systems have been employed for manipulation.<sup>6</sup> A number of approaches for creating nanochannels/nanopores have been reported,<sup>7</sup> including the standard photolithography with high-accuracy etching techniques,<sup>8–10</sup> the integration of commercially available membranes with nanopores,<sup>11–15</sup> and the employment of junction gap electric breakdown between two poly(dimethyl siloxane) (PDMS) microchannels.<sup>16,17</sup> However, standard photolithography is time-consuming and costly.<sup>18</sup> As for the strategy of using nanoporous membranes, although adopting photopolymerization might overcome the problem of liquid leakage, a complex optical setup and careful operation are required to complete the process.<sup>19</sup> When using a junction gap electric breakdown, however, a high direct-current (DC) voltage is required.<sup>16</sup> Our previous work<sup>20</sup> utilized nanoparticle (NP) deposition at the junction gap between microchannels to reduce the required electric breakdown voltage. The required voltage was only 36% of that without nanoparticle deposition. Furthermore, a self-assembled monolayer (SAM) of gold NPs (AuNPs) was employed to reduce the required voltage for electric breakdown.<sup>21</sup> The method for nanofracture formation involving the use of the SAMs of AuNPs at the junction gap between microchannels could be well controlled and was reliable. However, a voltage of hundreds of volts was still required. In the present study, a simple and novel protein preconcentrator is proposed. The exclusion-enrichment effect is achieved in nano-interstices via a self-assembled monolayer (SAM) of AuNPs. The proposed method does not require high-voltage or time-consuming fabrication. Meanwhile, it is very simple and reliable.

## II. EXPERIMENTAL SECTION

PDMS was adopted for fabricating the micro/nanofluidic channels in a chip for protein preconcentration. Two junction gaps were designed along the main microchannel for the formation of nano-interstices via the AuNP-based SAM. The layout and fabrication of the proposed protein preconcentrator herein are basically the same as those in our previous work,<sup>21</sup> which is shown in Figs. 1(a) and 1(b). The depth and width of the main microchannel are 2 and 100  $\mu\text{m}$ , respectively. The width of the junction gap is 50  $\mu\text{m}$ . To facilitate alignment during the bonding process of the PDMS replica with the glass substrate, the AuNP SAM region on the glass substrate was changed to 100  $\mu\text{m} \times 700 \mu\text{m}$  under the junction gaps and the vertical main microchannel to cover the junction gaps. The AuNP SAM region on the glass substrate was patterned using standard photolithography with an S1818 photoresist. Silanization on the glass substrate was achieved using 6  $\mu\text{l}$  of 0.1% v/v (3-aminopropyl)triethoxysilane/ $\text{H}_2\text{O}$  solution for 1 min. The glass substrate was then nitrogen-dried after being rinsed in deionized (DI) water and was then reacted for 1 h in 30  $\mu\text{l}$  of liquid containing AuNPs of various sizes (3, 13, and 40 nm in diameter) for self-assembly (Fig. 1(c)). Subsequently, the glass substrate underwent multiple rinses in acetone, methanol, and DI water to remove the photoresist. The AuNPs used in this study were purchased from Cytodiagnostics, Inc. (Burlington, Ontario, Canada). The SEM images of the SAM at 3, 13, and 40 nm are shown in Fig. 1(d). The results indicate that the layer of AuNP-based SAM is uniform and homogeneous. SEM analysis was performed on a HR-Scanning electron microscope with an energy-dispersive X-ray (EDX) spectrometer (JEOL JSM-6700F, Tokyo, Japan). After the AuNPs had self-assembled in the designated region, the PDMS replica was bonded to the glass substrate using oxygen-plasma treatment in an  $\text{O}_2$  plasma cleaner (PDC-32G, Harrick Plasma Corp., Ithaca, NY, USA). Four electrodes were then inserted into the reservoirs to apply the required voltage in the preconcentration experiments. Nanofluidic channels formed in the nano-interstices among the self-assembled AuNPs. The fabricated preconcentrator is also shown in Fig. 1(b).

## III. RESULTS AND DISCUSSION

Fluorescein isothiocyanate (FITC)-labeled bovine serum albumin (BSA) (Sigma-Aldrich, St. Louis, MO, USA) diluted in a 10 mM phosphate-buffered saline (PBS) solution to a concentration of 10  $\mu\text{M}$  was allowed to fill the microchannel via capillary force to demonstrate the on-chip protein preconcentration. The operational details of the electrokinetic protein preconcentration were presented in our previous work.<sup>22</sup> The depletion regions in the main vertical channel elongated

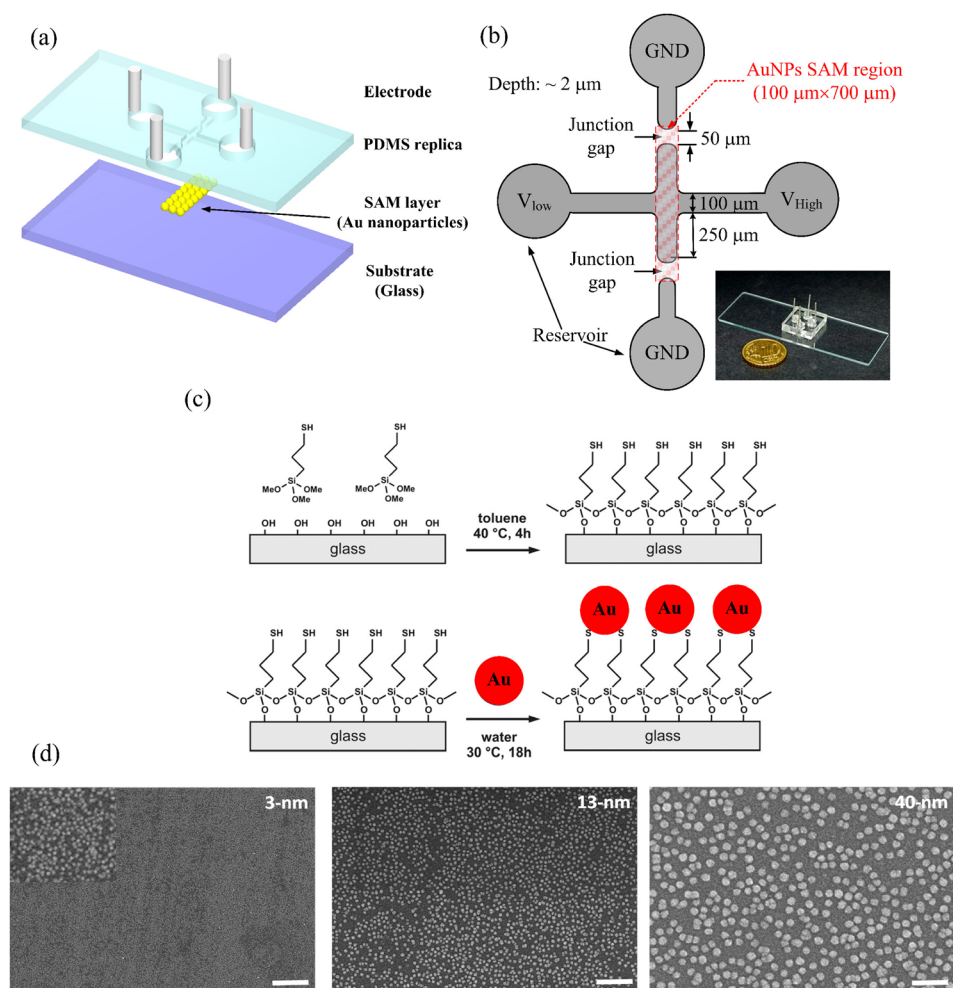


FIG. 1. The proposed chip with nanofluidic channels. (a) Schematic illustration (Adapted with permission from Jen *et al.*, PLoS One 10, e0126641 (2015). Copyright 2015 PLOS), (b) layout of protein preconcentrator with Au NP SAM (inset shows image of fabricated microchip), (c) gold nanoparticle self-assembly processes on the glass substrate, and (d) SEM images of the SAM with 3, 13, and 40-nm gold nanoparticles (scale bar is 200 nm).

when a DC voltage of 50 V was applied to the two anodic side reservoirs, while the other reservoirs were grounded. The elongated depletion regions from the top and bottom junction gaps merged and extended to the main horizontal channel. A bias voltage of 49 V was set on the left anodic side to induce electroosmotic flow (EOF) in order to accumulate proteins. Depletion forces were generated via the nano-interstices. Fluorescence images of 10  $\mu$ M FITC-labeled BSA in 10 mM PBS solution taken at various time points are shown in Fig. 2. The protein preconcentrator was fabricated with an SAM of 13-nm AuNPs. The experimental preconcentration results reveal that the concentration of BSA increased with time, which demonstrates that proteins can be successfully concentrated using the proposed preconcentrator. The concentration of the collected BSA proteins obtained from fluorescence intensity was quantified and averaged over a rectangular window (100  $\mu$ m  $\times$  300  $\mu$ m) using ImageJ software (National Institutes of Health, Bethesda, Maryland, USA), which can be used to assess the density of each pixel. The concentration performance for an initial protein concentration of 10  $\mu$ M is plotted in Fig. 3. To estimate the final concentration, the fluorescence intensity of the standard sample solution (1 mM proteins) was also measured. As shown in this figure, the results indicate that the 10  $\mu$ M protein sample was concentrated to approximately 1 mM in 30 min (approximately 100-fold the initial concentration), demonstrating the feasibility of the proposed approach. Solutions of 3- and 40-nm AuNPs, respectively, were also adopted for self-assembly on the glass substrate after silanization to

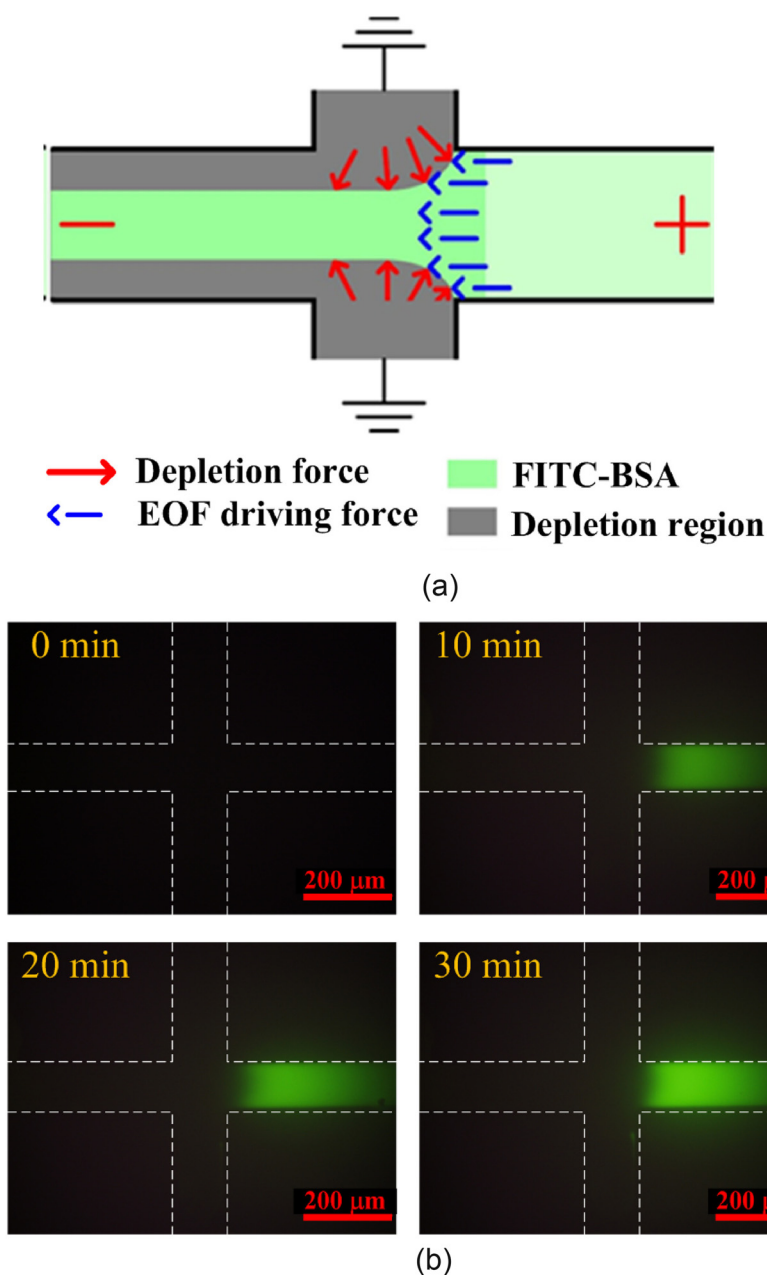


FIG. 2. Illustration and experimental results of electrokinetic protein preconcentration. (a) The schematic diagram for the depletion force elicited in nano-interstices among the self-assembled AuNPs and the EOF driving force. (b) Fluorescence images of 10  $\mu\text{M}$  FITC-labeled BSA in a 10 mM PBS solution taken at various time points. The preconcentrator was fabricated with an SAM of 13-nm AuNPs.

observe the effect of particle size. The fluorescence intensities after concentration for 30 min were quantified. These results, along with those for 13-nm AuNPs, are depicted in Fig. 4. The results show that only the SAM with 13-nm AuNPs achieved a successful protein concentration. In the experiments, no depletion force was generated when the 3-nm AuNPs were used, as shown in the left inset in Fig. 4. The experimental results indicate that 13-nm AuNPs provide suitable nano-interstices for protein concentration via the exclusion-enrichment effect. The reason for this is that it is possible that nanochannels through self-assembled AuNPs act as an ionic selective membrane due to the ion exclusion/enrichment effect caused by EDL overlap. When EDL overlap occurs inside a nanochannel with a negatively charged surface, the cation concentration will

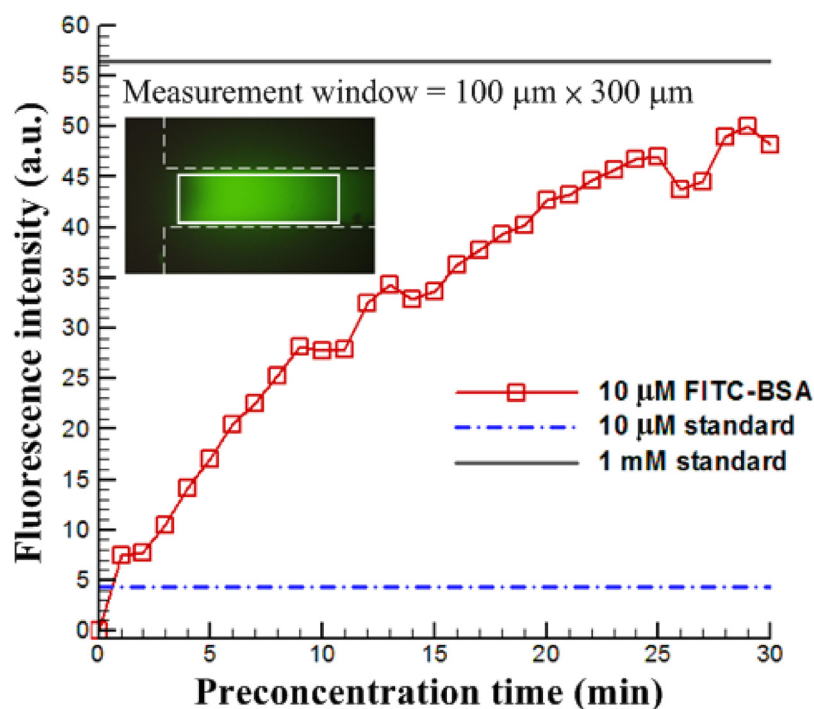


FIG. 3. Performance of concentrating the 10  $\mu\text{M}$  protein sample on the preconcentrator with an SAM of 13-nm AuNPs.

be greater than the anion concentration. That is, both positive and negative ions get depleted at the anode end and accumulate at the cathode end of the nanochannel, which is called ion concentration polarization. The existence and degree of EDL overlap are characterized by a comparison of the distance between opposite surfaces with the Debye length. Based on the Gouy-Chapman model, the Debye length is inversely proportional to the square root of the electrolyte concentration,<sup>23</sup> and that of a PDMS-based negative charge interface is approximately 3–5 nm for an

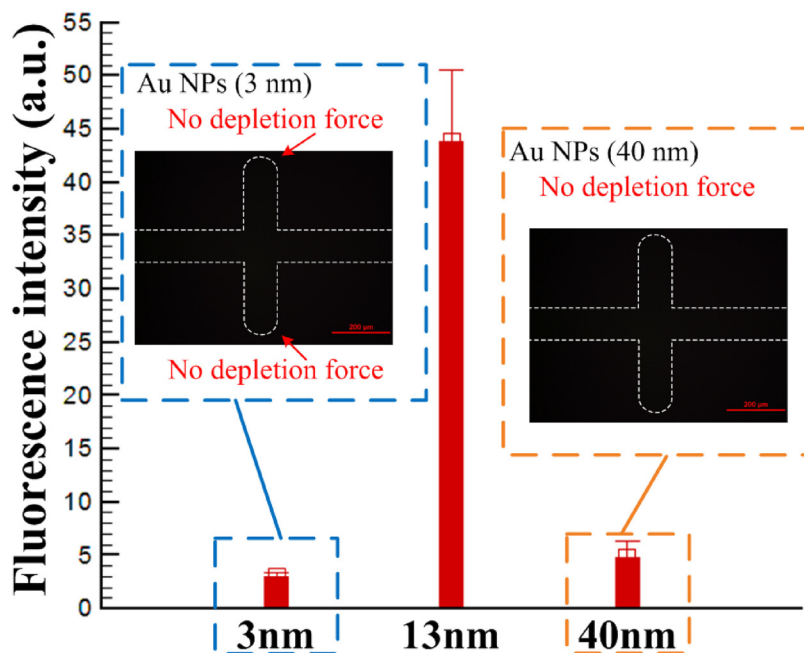


FIG. 4. Intensities of fluorescence for an SAM of AuNPs with various sizes after concentration for 30 min.



electrolyte concentration of 10 mM.<sup>24</sup> The fact that we observed is the formation of the ion depletion force reflects that the degree of EDL overlap depends on the SAM AuNP size. For nanochannels with a 13-nm AuNP SAM, the preconcentration effect occurs via the depletion force caused by a significant EDL overlap. However, for 3- and 40-nm AuNPs, no depletion effect was observed, indicating that the level of EDL overlap was too large or was non-existent, respectively. Furthermore, the small derivation of preconcentration efficiency under five replications reflects that the proposed fabrication process is reliable. To further prove that AuNPs were exactly sandwiched between the glass coverslip and the PDMS, ionic transport in nanochannels with a 13-nm AuNP SAM to be characterized by a significant enhancement in conductance relative to the bulk properties of the solution at low ionic strength, as shown in Fig. S1 of the supplementary material.<sup>25</sup> The bulk properties are predicted from the measured channel dimensions and the bulk solution conductivity. At high ionic strength, the measured conductance increased linearly with ionic strength, following the expected behavior. At low ionic strength, however, the measured channel conductance revealed a remarkable saturation that was independent of ionic strength. This is due to the increased surface-to-volume ratio in the nano-interstices and, therefore, to an increased contribution to the nanochannel conductivity from the surface charge. For the chip without SAM, otherwise, we measured a nearly constant conductance from high to low ionic strength. These results reflected that Au nanoparticles are exactly sandwiched between the glass coverslip and the PDMS channel wall to form nano-interstices. If the sandwiched structures did not form, the depletion force will not be consequently generated.

#### IV. CONCLUSIONS

In this work, a new fabrication of nanochannels for protein preconcentration devices was proposed. The nanofluidic channels were engineered through a self-assembled gold nanoparticle (AuNP) process. An effective depletion force is elicited in nano-interstices among self-assembled AuNPs due to the overlap of electrical double layers; therefore, proteins quickly accumulate. It was found that the depletion force can be manipulated by changing the sizes of the self-assembled gold nanoparticles. The experimental results showed that the self-assembled 13-nm AuNP monolayer can successfully preconcentrate proteins through effective EDL overlapping. This approach provides a new process to produce nanochannels through self-assembled gold nanoparticles and does not require high-voltage or time-consuming fabrication. Moreover, our experimental results indicated that the size of the AuNP employed in the SAM process is a crucial factor in this approach. Future experiments should investigate the detailed mechanisms of depletion force on the nanochannels formed by self-assembled gold nanoparticles. Such preconcentration systems could be integrated to immunoassay systems to enhance the detection limit and precision of biomedical applications.

#### ACKNOWLEDGMENTS

The authors would like to thank the National Science Council of the Republic of China, Taiwan, for its financial support of this research under the following Grant Nos.: MOST 104-2221-E-194-007- and MOST 104-2633-B-006-002-.

<sup>1</sup>K.-C. Wang, A. Kumar, S. J. Williams, N. G. Green, K. C. Kim, and H.-S. Chuang, *Lab Chip* **14**, 3958 (2014).

<sup>2</sup>J.-C. Wang, H.-Y. Ku, D.-B. Shieh, and H.-S. Chuang, *Biomicrofluidics* **10**, 014113 (2016).

<sup>3</sup>Q. Pu, J. Yun, H. Temkin, and S. Liu, *Nano Lett.* **4**, 1099 (2004).

<sup>4</sup>Y. Oh, H. Lee, S. Y. Son, S. J. Kim, and P. Kim, *Biomicrofluidics* **10**, 014102 (2016).

<sup>5</sup>A. Rohani, W. Varhue, Y.-H. Su, and N. S. Swami, *Biomicrofluidics* **8**, 052009 (2014).

<sup>6</sup>S. Song, A. K. Singh, and B. J. Kirby, *Anal. Chem.* **76**, 4589 (2004).

<sup>7</sup>C. Duan, W. Wang, and Q. Xie, *Biomicrofluidics* **7**, 026501 (2013).

<sup>8</sup>P. Mao and J. Han, *Lab Chip* **5**, 837 (2005).

<sup>9</sup>Y. C. Wang, A. L. Stevens, and J. Han, *Anal. Chem.* **77**, 4293 (2005).

<sup>10</sup>T. Leichlé and C.-F. Chou, *Biomicrofluidics* **9**, 034103 (2015).

<sup>11</sup>J. H. Lee, Y.-A. Song, and J. Han, *Lab Chip* **8**, 596 (2008).

<sup>12</sup>J. K. Sung and J. Han, *Anal. Chem.* **80**, 1529 (2008).

<sup>13</sup>D. Wu and A. J. Steckl, *Lab Chip* **9**, 1890 (2009).

<sup>14</sup>R.-J. Yang, H.-H. Pu, and H.-L. Wang, *Biomicrofluidics* **9**, 014122 (2015).

- <sup>15</sup>Y.-Y. Chen, P.-H. Chiu, C.-H. Weng, and R.-J. Yang, *Biomicrofluidics* **10**, 014119 (2016).
- <sup>16</sup>H. L. Jeong, S. Chung, J. K. Sung, and J. Han, *Anal. Chem.* **79**, 6868 (2007).
- <sup>17</sup>S. M. Kim, M. A. Burns, and E. F. Hasselbrink, *Anal. Chem.* **78**, 4779 (2006).
- <sup>18</sup>C. C. Lin, J. L. Hsu, and G. B. Lee, *Microfluid. Nanofluid.* **10**, 481 (2011).
- <sup>19</sup>H. Yu, Y. Lu, Y. Zhou, F. Wang, F. He, and X. Xia, *Lab Chip* **8**, 1496 (2008).
- <sup>20</sup>C.-P. Jen, T. G. Amstislavskaya, C.-C. Kuo, and Y.-H. Chen, *PLoS One* **9**, e102050 (2014).
- <sup>21</sup>C.-P. Jen, T. G. Amstislavskaya, K.-F. Chen, and Y.-H. Chen, *PLoS One* **10**, e0126641 (2015).
- <sup>22</sup>P.-J. Chiang, C.-C. Kuo, T. N. Zmay, A. S. Zmay, and C.-P. Jen, *Microelectron. Eng.* **115**, 39 (2014).
- <sup>23</sup>J. N. Israelachvili, *Intermolecular and Surface Forces* (Elsevier, 2011).
- <sup>24</sup>A. Sze, D. Erickson, L. Ren, and D. Li, *J. Colloid Interface Sci.* **261**, 402 (2003).
- <sup>25</sup>See supplementary material at <http://dx.doi.org/10.1063/1.4946768> for measured DC conductances for the nano-interstice of AuNP SAM between the junction gap.